

# Synthesis, structural characterization and biological studies of copper complexes with 2-aminobenzothiazole derivatives



J. Joseph\*, G. Boomadevi Janaki

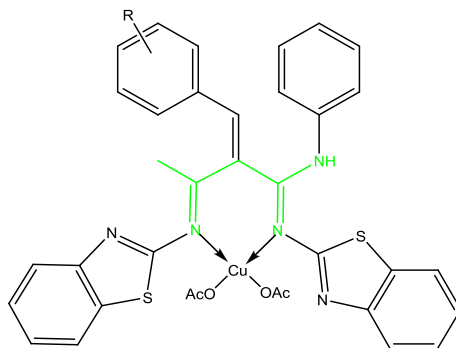
Department of Chemistry, Noorul Islam Centre for Higher Education, Kumaracoil 629180, Tamil Nadu, India

## HIGHLIGHTS

- A series of novel copper complexes of 2-aminobenzothiazole derivatives were synthesized.
- A potent lead compound by selecting suitably substituted Knoevenagel moiety.
- Six compounds with high potency and better antioxidant agents.

## GRAPHICAL ABSTRACT

Novel copper complexes of 2-aminobenzothiazole derivatives were synthesized by the condensation of Knoevenagel condensate acetoacetanilide (obtained from substituted benzaldehydes and acetoacetanilide) and 2-aminobenzothiazole. They were thoroughly characterized by elemental analysis, IR, <sup>1</sup>H NMR, UV-Vis., molar conductance, magnetic moment and electrochemical studies.



## ARTICLE INFO

### Article history:

Received 5 October 2013

Received in revised form 9 January 2014

Accepted 10 January 2014

Available online 28 January 2014

### Keywords:

2-aminobenzothiazole

Characterization

Pharmacological and biological

## ABSTRACT

Novel copper complexes of 2-aminobenzothiazole derivatives were synthesized by the condensation of Knoevenagel condensate acetoacetanilide (obtained from substituted benzaldehydes and acetoacetanilide) and 2-aminobenzothiazole. They were thoroughly characterized by elemental analysis, IR, <sup>1</sup>H NMR, UV-Vis., MS Spectra, molar conductance, magnetic moment and electrochemical studies. These spectral studies suggested that distorted square planar geometry for all the complexes. Molar conductance data and magnetic susceptibility measurements provide evidence for monomeric and neutral nature of the complexes. The electrochemical behaviour of the ligand and complexes in DMSO at 298 K was studied. The present ligand systems stabilize the unusual oxidation states of copper ion during electrolysis. Antibacterial screening of the ligands and their complexes reveal that all the complexes show higher activities than the free ligands.

© 2014 Elsevier B.V. All rights reserved.

## 1. Introduction

Innovations/Inventions of newer, cheaper and more potent analogs of molecules with already well recognized biological

activities from a key part of research in the pharmaceutical field. Bring about modifications by manipulating the parent structures serves to enhance the activity of the potent analogs and eliminates adverse effects or toxicity associated with the parent drug. Particularly, 2-aminobenzothiazole/beta-diketone and its derivatives are known for their variety of clinical applications [1–3].

\* Corresponding author. Tel.: +91 9629474150.

E-mail address: [Chem\\_joseph@yahoo.co.in](mailto:Chem_joseph@yahoo.co.in) (J. Joseph).

In this present study, we have focused on the structural modifications on 2-aminobenzothiazole. In this perspective, low molecular weight transition metal complexes with organic ligands have been and are still viewed as promising pharmaceutical agents with antioxidant/free radical scavenging properties, owing to their ability to interact and/or react with reactive oxygen or nitrogen species and counterbalance excessive endogenous free radical generation in biological systems. It is hope that metal complexes may be behaved as therapeutics.

The  $\beta$ -diketones such as curcumin, phloretin and structurally related phytopolyphenols have well described neuroprotective properties against toxicity induced by hydrogen peroxide in a cellular model of oxidative stress [4]. Among them curcumin has crucial features of a neuroprotective drug since it acts as a powerful scavenger of superoxide anions so it has both neuroprotective and anti-aging effects. Thus, the curcumin based analogs have great potential for the prevention of multiple neurological conditions than the current therapeutics [5]. Condensation of the active methylene group of the  $\beta$ -diketone with an aldehydic group will give a non-enolisable Knoevenagel condensate, which can effectively react with amines to form Schiff bases. Schiff bases have been reported to show a variety of biological activities like antibacterial, antifungal, herbicidal and clinical activities by virtue of the azomethine linkage [6].

Benzothiazoles are bicyclic ring system with multiple applications. Among benzothiazoles, 2-aryl benzothiazole has received much attention due to unique structure and an important pharmacophore in a number of diagnostic and therapeutic agents which was studied at 1950s. It is used as radioactive amyloid imaging agents [7] and anticancer agents [8] and reported cytotoxic on cancer cells [9]. Polyfunctional ligands system of 2-aminobenzothiazoles has been studied as central muscle relaxants and are found to interfere with glutamate neurotransmission in biochemical, electrophysiological and behavioural experiments and reported as neuroprotectors [10]. Some of these drugs exhibit increased anticancer activity when administered as metal complexes [11,12]. Metal complexes of N and S chelating ligands have attracted considerable attention because of their interesting physicochemical properties and pronounced biological and pharmacological activities. The N and S atoms play a key role in the coordination of metals at the active sites of various metallobiomolecules [13,14].

Copper is an important biometal which is essential for normal human metabolism and its imbalance leads to deficiency or excess diseases. Cu(II) complexes are preferred candidates for various pharmacological studies due to the presence of its biorelevant ligands [15]. These complexes have multiple roles in medicinal proceedings such as antimicrobial, antiviral, anti-inflammatory, antitumor agents, enzyme inhibitors, or chemical nucleases with reduced side effects and it has distinct superoxide-dismutase-(SOD-)mimetic activity [16,17]. DNA is a potent target of cytostatic drugs, the effect of copper compounds on DNA functionality is very important. The ability of Cu(II) complexes to bind to DNA and exhibit nuclease activity in the presence of reducing agents is well established [18].

Literature review shows that heterocyclic derivatives containing nitrogen and sulphur atom serve as a unique and versatile scaffolds for systematic drug design. These concerns have led to major research efforts to discover new antibacterial agents that could be used to combat bacterial infections one of which are the Schiff bases have highly conjugated Pharmacophoric systems. Based upon this we synthesized a series of copper complexes from the Schiff base ligands synthesized by the condensation of Knoevenagel condensate acetoacetanilide (obtained from substituted benzaldehydes and acetoacetanilide). The synthesized ligand system is highly conjugated like curcumin (Scheme 1) analog so we are promising that nitrogen and sulphur containing heterocycles have

pronounced biological and pharmacological activities. As a consequence, it is essential to understand the relationship between ligand and the copper ion in biological systems. We have undertaken intensive efforts to synthesize and present them as a potential candidate for neuronal diseases. The aim of the present study is to prepare the desired Schiff bases which are based on the condensation of a Knoevenagel condensate of acetoacetanilide precursor with 2-aminobenzothiazole and to investigate their effect on pathogenic strains of Gram-positive and Gram-negative bacteria. Further, *in vitro* free radical scavenging activities of the ligands and their copper complexes were evaluated by DPPH assay method. The DNA binding efficiency of copper complexes has also been determined using electrochemical and electronic absorption techniques.

## 2. Experimental

### 2.1. Material

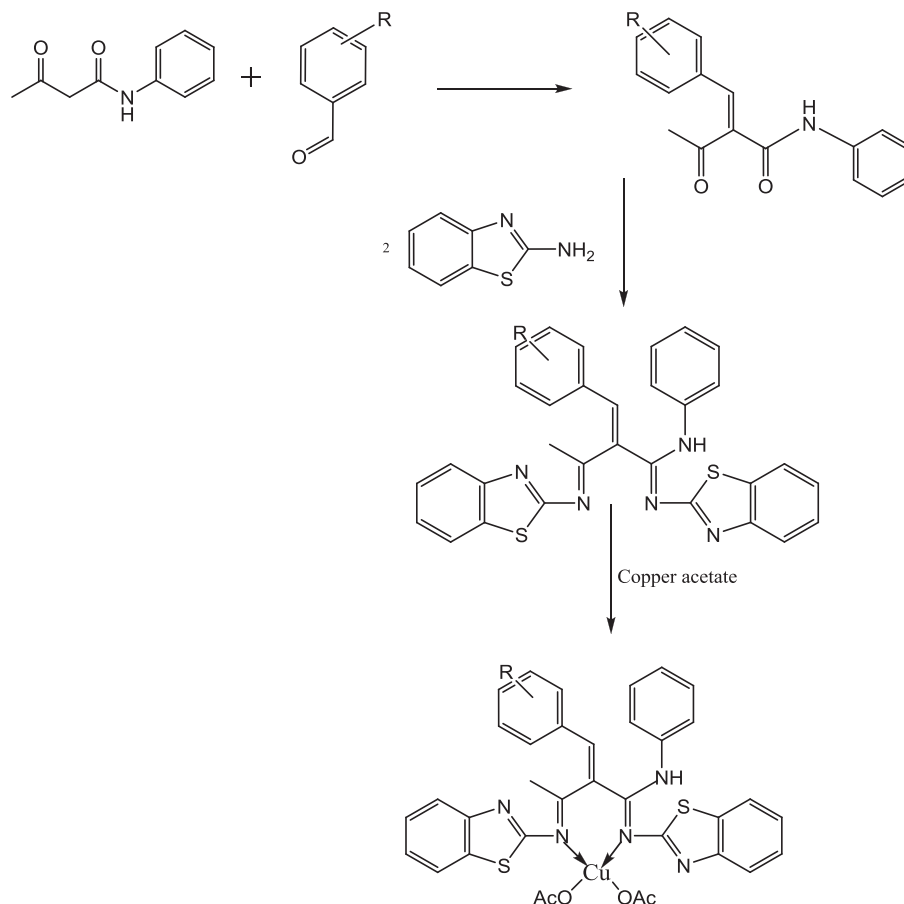
All chemicals and solvents were reagent grade and were purchased from Merck. All supporting electrolyte solutions were prepared using analytical grade reagents and doubly distilled water. Calf thymus DNA purchased from Genei Biolab, Bangalore, India.

### 2.2. Instrumentation

Elemental analysis of ligands and their copper complexes were carried out using Perkin–Elmer elemental analyzer. Molar conductance of the complexes was measured using a coronation digital conductivity meter. The  $^1\text{H}$  NMR spectra of the ligands were recorded using TMS as internal standard. Chemical shifts are expressed in units of parts per million relative to TMS. The IR spectra of the ligands and their copper complexes were recorded on a Perkin–Elmer 783 spectrophotometer in  $4000\text{--}200\text{ cm}^{-1}$  range using KBr disc. Electronic spectra were recorded in a Systronics 2201 Double beam UV–Vis., spectrophotometer within the range of  $200\text{--}800\text{ nm}$  region. Magnetic moments were measured by Guoy method and corrected for diamagnetism of the component using Pascal's constants. Cyclic voltammetry was performed on a CHI 604D electrochemical analyzer with three electrode system of glassy carbon as the working electrode, a platinum wire as auxiliary electrode and Ag/AgCl as the reference electrode. Tetraabutylammoniumperchlorate (TBAP) was used as the supporting electrolyte. Solutions were deoxygenated by eradication with  $\text{N}_2$  previous to measurements. The interactions between metal complexes and DNA were studied using electrochemical and electronic absorption techniques. The FAB-mass spectra of ligands and their metal complexes were recorded on a JEOL SX 102/DA-6000 mass spectrometer/data system using Argon/Xenon (6 kV, 10 A) as the FAB gas. The Thermogravimetric analyses data were measured from  $0\text{ }^\circ\text{C}$  to  $1000\text{ }^\circ\text{C}$  temperature at a heating rate of  $10\text{ }^\circ\text{C}/\text{min}$ . The data were obtained by using a Perkin Elmer Diamond TG/DTA instrument.

### 2.3. Synthesis of Knoevenagel condensate $\beta$ -diketones

The reaction was proceeded by Knoevenagel condensation between equimolar quantity of acetoacetanilide and aromatic aldehyde(s) such as 4-hydroxy-3-methoxybenzaldehyde ( $\text{L}^1$ )/4-chlorobenzaldehyde ( $\text{L}^2$ )/3-nitrobenzaldehyde ( $\text{L}^3$ )/2-chlorobenzaldehyde ( $\text{L}^4$ )/3-chlorobenzaldehyde ( $\text{L}^5$ )/cinnamaldehyde ( $\text{L}^6$ ) was refluxed in the presence of potassium carbonate as the catalyst. The product was formed with loss of water molecule to provide substituted  $\beta$ -ketoanilides. The progress of reaction was monitored by TLC. After completion of reaction, the reaction mixture was poured on



**Scheme 1.** Outline of synthesis of copper complexes of 2-aminobenzothiazole derivatives.

crushed ice. The yellow coloured Knoevenagel condensate β-ketoanilide was obtained. The separated product was filtered washed with ice cold water and dried.

#### 2.4. Synthesis of Schiff base ligands

Ethanol solutions of 2 mol of 2-aminobenzothiazole was added dropwise to one mole of Knoevenagel condensate β-ketoanilide(s) in 40 ml ethanol and anhydrous potassium carbonate used as a catalyst. The obtained products were set aside in a refrigerator for 10 h. The progress of reaction was monitored by TLC. After completion of reaction the solid material was removed by filtration and recrystallized from ethanol. The better percentage yield (75%) was obtained by adopting the above procedure.

#### 2.5. Synthesis of copper(II) complexes

Ethanol solutions of 2-aminobenzothiazole derivatives (2 mol) and copper acetate (1 mol) were refluxed for about 2 h. The progress of reaction was monitored by TLC until the product was formed. Then, it was poured on crushed ice. The solid material was removed by filtration and recrystallized from ethanol.

The following schematic representation shows the outline of synthesis of compounds and their complexes.

#### 2.6. DNA binding studies

The binding interactions between metal complexes and DNA were studied using electrochemical and electronic absorption methods by using different concentrations of CT-DNA. Solutions

of CT DNA in 50 mM NaCl/50 mM tris-HCl (pH 7.2) gave the ratio of the UV absorbance at 260 and 280 nm,  $A_{260}/A_{280}$ , of ca. 1.8–1.9, indicating that the DNA was sufficiently free of protein contamination. The DNA concentration was determined by the UV absorbance at 260 nm after 1:100 dilution. The molar absorption coefficient was taken as  $6600 \text{ m}^2 \text{ mol}^{-1}$ . Stock solutions were kept at 4 °C and used safter not more than 4 days. Concentrated stock solutions of the complexes were prepared by dissolving the complexes in DMSO and diluting suitably with the corresponding buffer to the required concentration for all of the experiments.

##### 2.6.1. Absorption titration experiment

Absorption titration experiment was performed by maintaining a constant concentration of the complex while varying the nucleic acid concentration. This was achieved by dissolving an appropriate amount of the copper complex stock solution and by mixing various amounts of DNA stock solutions while maintaining the total volume constant. This resulted in a series of solutions with varying concentrations of DNA but with a constant concentration of the complex. The absorbance ( $A$ ) of the most red-shifted band of complex was recorded after each successive additions of CT DNA. The intrinsic binding constant,  $K_b$ , was determined from the plot of  $[\text{DNA}]/(\epsilon_a - \epsilon_f)$  vs  $[\text{DNA}]$ , where  $[\text{DNA}]$  is the concentration of DNA in base pairs,  $\epsilon_a$ , the apparent extinction coefficient which is obtained by calculating  $A_{\text{obs}}/[\text{complex}]$  and  $\epsilon_f$  corresponds to the extinction coefficient of the complex in its free form. The data were fitted to the following equation where  $\epsilon_b$  refers to the extinction coefficient of the complex in the fully bound form.

$$[\text{DNA}]/(\epsilon_a - \epsilon_f) = [\text{DNA}]/(\epsilon_b - \epsilon_f) + 1/K_b(\epsilon_b - \epsilon_f) \quad (1)$$

Each set of data, when fitted to the above equation, gave a straight line with a slope of  $1/(\epsilon_b - \epsilon_f)$  and a y-intercept of  $1/K_b(\epsilon_b - \epsilon_f)$ .  $K_b$  was determined from the ratio of the slope to intercept.

## 2.7. Antioxidant Assay

### 2.7.1. Superoxide dismutase activity (SOD)

The superoxide dismutase activity (SOD) of the copper(II) complexes were evaluated using alkaline DMSO as source of superoxide radicals ( $O_2^{\cdot-}$ ) generating system in association with nitro blue tetrazolium chloride (NBT) as a scavenger of superoxide. Add 2.1 ml of 0.2 M potassium phosphate buffer (8.6 pH) and 1 ml of 56  $\mu$ l of NBT solutions to the different concentration of copper complex solution. The mixtures were kept in ice for 15 min and then 1.5 ml of alkaline DMSO solution was added while stirring. The absorbance was monitored at 540 nm against a sample prepared under similar condition except NaOH in DMSO.

### 2.7.2. Hydrogen peroxide assay

A solution of hydrogen peroxide (2.0 Mm) was prepared in phosphate buffer (0.2 M, 7.4 pH) and its concentration was determined spectrophotometrically from absorption at 230 nm. The complexes of different concentration and Vitamin C (100  $\mu$ g/ml) were added to 3.4 ml of phosphate buffer together with hydrogen peroxide solution (0.6 ml). An identical reaction mixture without the sample was taken as negative control. The absorbance of hydrogen peroxide at 230 nm was determined after 10 min against the blank (phosphate buffer).

## 2.8. Antimicrobial activities

The *in vitro* antimicrobial activities of the investigated compounds were tested against the bacterial species and fungal species. One day prior to the experiment, the bacterial and fungal cultures were inoculated in broth (inoculation medium) and

incubated overnight at 37 °C. Inoculation medium containing 24 h grown culture was added aseptically to the nutrient medium and mixed thoroughly to get the uniform distribution. This solution was poured (25 mL in each dish) into petri dishes and then allowed to attain room temperature. Wells (6 mm in diameter) were cut in the agar plates using proper sterile tubes. Then, wells were filled up to the surface of agar with 0.1 mL of the test compounds dissolved in DMSO (200  $\mu$ M/mL). The plates were allowed to stand for an hour in order to facilitate the diffusion of the drug solution. Then the plates were incubated at 37 °C for 24 h for bacteria and 48 h for fungi and the diameter of the inhibition zones were read. Minimum inhibitory concentrations (MICs) were determined by using serial dilution method. The lowest concentration ( $\mu$ g/mL) of compound, which inhibits the growth of bacteria after 24 h incubation at 37 °C. The concentration of DMSO in the medium did not affect the growth of any of the microorganisms tested.

## 3. Results and discussion

The ligands and their complexes are stable at room temperature. Copper complexes are stable at room temperature and do not undergo any decomposition for a long time. They are sparingly soluble in common organic solvents but soluble in DMF and DMSO. The analytical, physical properties and molar conductance data of the complexes are given in Table 1. The Cu(II) complexes were dissolved in DMSO and the molar conductivities of  $10^{-3}$  M of their solution at room temperature were measured. The lower conductance values ( $2\text{--}5 \Omega^{-1} \text{cm}^2 \text{mol}^{-1}$ ) of the complexes support their non-electrolytic nature. Thus, the present complexes have non-electrolytic nature as evidenced by the involvement of acetate ions in coordination. This result was further confirmed from the chemical analysis of  $\text{CH}_3\text{COO}^-$  ion, not precipitated by addition of  $\text{FeCl}_3$ . The elemental analysis data of the complexes are in good agreement with theoretical values presented in Table 1. The results obtained from micro analytical measurements, metal estimation,

**Table 1**

Physical characterization, analytical, molar conductance and magnetic susceptibility data of the ligands and their complexes.

Compound	Yield (%)	Colour	(Found) calc				$(\Omega^{-1} \text{cm}^2 \text{mol}^{-1})$	$\mu_{\text{eff}}$ (BM)
			Cu	C	H	N		
L <sup>1</sup>	62	Dark brown	–	68.31 (68.12)	4.66 (4.37)	9.96 (9.88)	–	–
L <sup>2</sup>	73	Dark brown	–	67.69 (67.87)	4.03 (3.82)	10.19 (10.06)	–	–
L <sup>3</sup>	76	Dark brown	–	66.06 (66.12)	4.47 (4.67)	12.43 (12.88)	–	–
L <sup>4</sup>	54	Dark brown	–	67.69 (67.87)	4.03 (3.82)	10.19 (10.06)	–	–
L <sup>5</sup>	43	Dark Brown	–	67.69 (67.87)	4.03 (3.82)	10.19 (10.06)	–	–
L <sup>6</sup>	65	Yellow	–	74.28 (74.06)	4.68 (4.41)	8.69 (8.49)	–	–
[CuL <sup>1</sup> (OAc) <sub>2</sub> ]	56	Reddish brown	8.56 (8.43)	58.17 (58.43)	4.21 (4.06)	7.54 (7.45)	3	1.82
[CuL <sup>2</sup> (OAc) <sub>2</sub> ]	74	Pale brown	8.69 (8.60)	57.44 (57.53)	3.86 (3.92)	7.66 (7.51)	4	1.80
[CuL <sup>3</sup> (OAc) <sub>2</sub> ]	78	Black	8.41 (8.98)	55.58 (32.73)	3.73 (2.43)	11.2 (6.43)	2	1.89
[CuL <sup>4</sup> (OAc) <sub>2</sub> ]	44	Pale brown	8.69 (8.60)	57.44 (57.53)	3.86 (3.92)	7.66 (7.51)	4	1.82
[CuL <sup>5</sup> (OAc) <sub>2</sub> ]	62	Pale brown	8.69 (8.60)	57.44 (57.53)	3.86 (3.92)	7.66 (7.51)	4	1.82
[CuL <sup>6</sup> (OAc) <sub>2</sub> ]	71	Light black	7.57 (7.42)	64.30 (64.43)	4.32 (4.16)	6.67 (6.87)	5	1.86

conductivity and mass spectral data confirm the stoichiometry of the copper complex as  $[\text{CuL}(\text{OAc})_2]$ . The magnetic moments of copper(II) in any of its geometry lies around 1.9 B.M. which is very close to spin-only value i.e. 1.73 B.M. The values which we found in our case lie in the range, 1.80–1.89 B.M. These values are typical for mononuclear copper(II) compounds having  $d^9$ -electronic configuration. The observed magnetic moments of all the complexes correspond to distorted square planar Cu(II) complexes. However, the values are slightly higher than the expected spin-only values due to spin orbit coupling contribution.

### 3.1. $^1\text{H}$ NMR

The  $^1\text{H}$  NMR spectra of ligands were recorded in DMSO- $d_6$  Solution at room temperature. The ligand  $L^1$  showed the following spectral features for Knoevenagel condensate acetoacetanilide moiety: aromatic protons of acetoacetanilide ring appear as multiplet at the region between 6.8–7.4  $\delta$ ppm (m, 5H), the phenyl multiplet was observed at 7.32–7.7 (m, 3H), methyl protons at 2.25 ppm (s, 3H),  $-\text{OH}$  at 10.8 (s, H) and  $-\text{OCH}_3$  at 3.5 (s, 3H). In addition, peak appeared at 7.3 ppm, which is assigned to free-NH group of acetoacetanilide moiety. Moreover the multiplets within the range 7.8–8.2 ppm (m, 8H) were assigned to the aromatic protons of benzothiazole ring [19]. The peak at 5.4 ppm is attributable to the  $-\text{HC}=\text{C}-$  group present in the Knoevenagel condensate moiety. The chemical shifts of all ligands are listed in Table 2. It was concluded that the absence of amino group of 2-aminobenzothiazole indicated the formation of schiff base ligand system.

### 3.2. FT-IR spectroscopy

In order to characterize the binding mode of the Schiff base to the metal ion in the complexes, the IR spectrum of the free ligand was compared with the spectra of the copper complexes. The characteristic IR bands for the synthesized ligands and their copper complexes were listed in Table 3. The IR Spectrum of  $[\text{CuL}^2(\text{OAc})_2]$  complex was shown in Fig. 1 as supplementary material. The spectrum of the ligand ( $L^2$ ) showed band at  $1646\text{ cm}^{-1}$  for the imine  $\nu(\text{C}=\text{N})$  group which results from the Schiff base condensation of 2-aminobenzothiazoles and Knoevenagel condensate was shifted to a lower frequency of  $1626\text{ cm}^{-1}$  after complexation [20]. Moreover, the appearance of new bands at  $451\text{ cm}^{-1}$  and  $510\text{ cm}^{-1}$  corresponds to  $\nu(\text{M}-\text{N})$  and  $\nu(\text{M}-\text{O})$  [21]. Also the new bands at  $1383\text{ cm}^{-1}$  and  $1292\text{ cm}^{-1}$  corresponds to symmetric and asymmetric stretching for  $\nu(\text{M}-\text{O})$  which evidenced the participation of the  $\text{COO}^-$  ion in the complexes. These facts are further supported by the appearance of bands between  $1390$ – $1456\text{ cm}^{-1}$  and  $1280$ – $1321\text{ cm}^{-1}$  attributed to  $\nu_{\text{asy}}(\text{COO}^-)$  and  $\nu_{\text{sy}}(\text{COO}^-)$  respectively in all copper complexes. The difference in  $\Delta\nu$  between  $\nu_{\text{asy}}(\text{COO}^-)$  and  $\nu_{\text{sy}}(\text{COO}^-)$  in metal complexes was  $\sim 100\text{ cm}^{-1}$  ( $110$ – $135\text{ cm}^{-1}$ ) suggests the mode of coordination of carboxylate group in copper complexes in a monodentate manner. Finally it was reported that the copper complexes were behave as bidentate and coordinate through azomethine nitrogen atoms and acetate ions.

**Table 2**  
 $^1\text{H}$  NMR chemical shifts  $\delta$  (ppm) of ligands  $L^1$ – $L^6$ .

Compound	$-\text{CH}_3$	$-\text{NH}$	Acetoacetanilide (aromatic)	Phenyl (aromatic)	Benzothiazole (aromatic)	Functional group
$L^1$	2.25	7.3	6.8–7.4	7.32–7.7	7.8–8.2	10.8 ( $-\text{OH}$ )
$L^2$	2.23	7.35	6.84–7.43	7.33–7.73	7.83–8.24	3.5 ( $\text{OCH}_3$ )
$L^3$	2.27	7.38	6.87–7.45	7.36–7.81	7.86–8.27	–
$L^4$	2.22	7.34	6.83–7.45	7.34–7.74	7.82–8.24	–
$L^5$	2.24	7.36	6.82–7.42	7.35–7.73	7.84–8.23	–
$L^6$	2.26	7.33	6.86–7.44	7.35–7.77	7.85–8.25	–

**Table 3**

Characteristic IR bands of the Schiff base ligands and their copper complexes (in  $\text{cm}^{-1}$ ).

Compound	$\nu$ ( $\text{C}=\text{N}$ )	$\nu$ ( $\text{C}=\text{N}$ )	$\nu$ ( $\text{M}-\text{O}$ )	$\nu$ ( $\text{M}-\text{N}$ )	$\nu_{\text{asy}}(\text{COO}^-)$	$\nu_{\text{sy}}(\text{COO}^-)$
$L^1$	1628	1642	–	–	–	–
$L^2$	1630	1646	–	–	–	–
$L^3$	1624	1662	–	–	–	–
$L^4$	1630	1653	–	–	–	–
$L^5$	1630	1652	–	–	–	–
$L^6$	1638	1666	–	–	–	–
$[\text{CuL}^1(\text{OAc})_2]$	1612	1624	510	449	1394	1298
$[\text{CuL}^2(\text{OAc})_2]$	1618	1626	509	451	1390	1294
$[\text{CuL}^3(\text{OAc})_2]$	1611	1618	507	452	1438	1321
$[\text{CuL}^4(\text{OAc})_2]$	1618	1626	509	451	1456	1308
$[\text{CuL}^5(\text{OAc})_2]$	1618	1631	510	453	1412	1280
$[\text{CuL}^6(\text{OAc})_2]$	1621	1632	512	448	1422	1317

The IR Spectral features were reinforced the conclusion drawn from conductance measurements [22].

### 3.3. Electronic spectroscopy

The electronic absorption spectra of the Schiff base ligands and their copper complexes in DMSO as a solvent were recorded at room temperature and the band positions of the absorption maxima; band assignments and the proposed geometry are mentioned in Table 4. The absorption spectrum for ligand  $L^2$  shows band at 329 nm attributed to  $\pi-\pi^*$  transitions within the Schiff base molecule. The electronic spectrum of the corresponding complex  $[\text{CuL}^2(\text{OAc})_2]$  (Fig. 2) in DMSO reveals a broad band at 429 nm assigned to  $^2\text{B}_{1g} \rightarrow ^2\text{A}_{1g}$  transition which is characteristic of distorted square planar environment around the copper(II) ion. Similar spectral features were assigned for other complexes [23].

**Table 4**  
Electronic spectra of Schiff base ligands and their copper complexes (nm).

Compound	Wavelength(nm)	Band assignments	Geometry
$L^1$	352	$\pi-\pi^*$	–
$L^2$	329	$\pi-\pi^*$	–
$L^3$	344	$\pi-\pi^*$	–
$L^4$	319	$\pi-\pi^*$	–
$L^5$	319	$\pi-\pi^*$	–
$L^6$	332	$\pi-\pi^*$	–
$[\text{CuL}^1(\text{OAc})_2]$	427	$^2\text{B}_{1g} \rightarrow ^2\text{A}_{1g}$	Distorted square planar
$[\text{CuL}^2(\text{OAc})_2]$	429	$^2\text{B}_{1g} \rightarrow ^2\text{A}_{1g}$	Distorted square planar
$[\text{CuL}^3(\text{OAc})_2]$	426	$^2\text{B}_{1g} \rightarrow ^2\text{A}_{1g}$	Distorted square planar
$[\text{CuL}^4(\text{OAc})_2]$	424	$^2\text{B}_{1g} \rightarrow ^2\text{A}_{1g}$	Distorted square planar
$[\text{CuL}^5(\text{OAc})_2]$	432	$^2\text{B}_{1g} \rightarrow ^2\text{A}_{1g}$	Distorted square planar
$[\text{CuL}^6(\text{OAc})_2]$	430	$^2\text{B}_{1g} \rightarrow ^2\text{A}_{1g}$	Distorted square planar

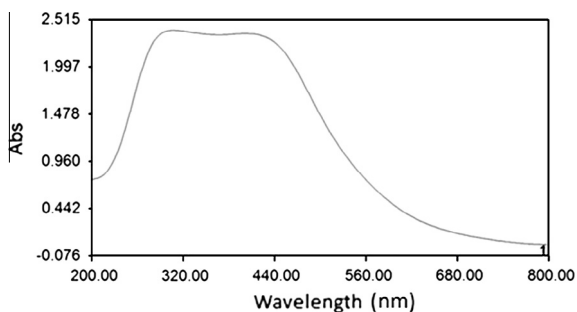


Fig. 2. Electronic absorption spectra of  $[\text{CuL}^2(\text{OAc})_2]$  complex.

### 3.4. EPR spectra

EPR spectrum of the copper complex was recorded in DMSO at 300 and 77 K. The spectrum at 300 K shows an intense absorption band at high field, which is isotropic due to tumbling motion of the molecules. This complex in the frozen state shows four well resolved peaks with low intensities in low field region. This fact was evident from the absence of half field signal, observed in the spectrum at 1600G due to the  $\Delta m_s = \pm 2$  transitions, ruling out any Cu–Cu interaction [24] and the synthesized compounds monomeric in nature [25]. The observed trend of copper complex of  $L^1$  is,  $g_{\parallel}(2.24) > g_{\perp}(2.05) > g_e(2.0023)$  describes the axial symmetry with the unpaired electron residing in the  $d_{x^2-y^2}$  orbital [26]. Molecular orbital coefficients  $\alpha^2$  (covalent inplane  $\sigma$ -bonding),  $\beta^2$  (covalent in-plane  $\pi$ -bonding) and  $\gamma^2$  (out-plane  $\pi$ -bonding) were calculated using the following Eqs. (2)–(4).

$$\alpha^2 = (A_{\parallel}/0.036) + (g_{\parallel} - 2.0027) + 3/7(g_{\perp} - 2.0023) + 0.04 \quad (2)$$

$$\beta^2 = (g_{\parallel} - 2.0027)E / -8\lambda\alpha^2 \quad (3)$$

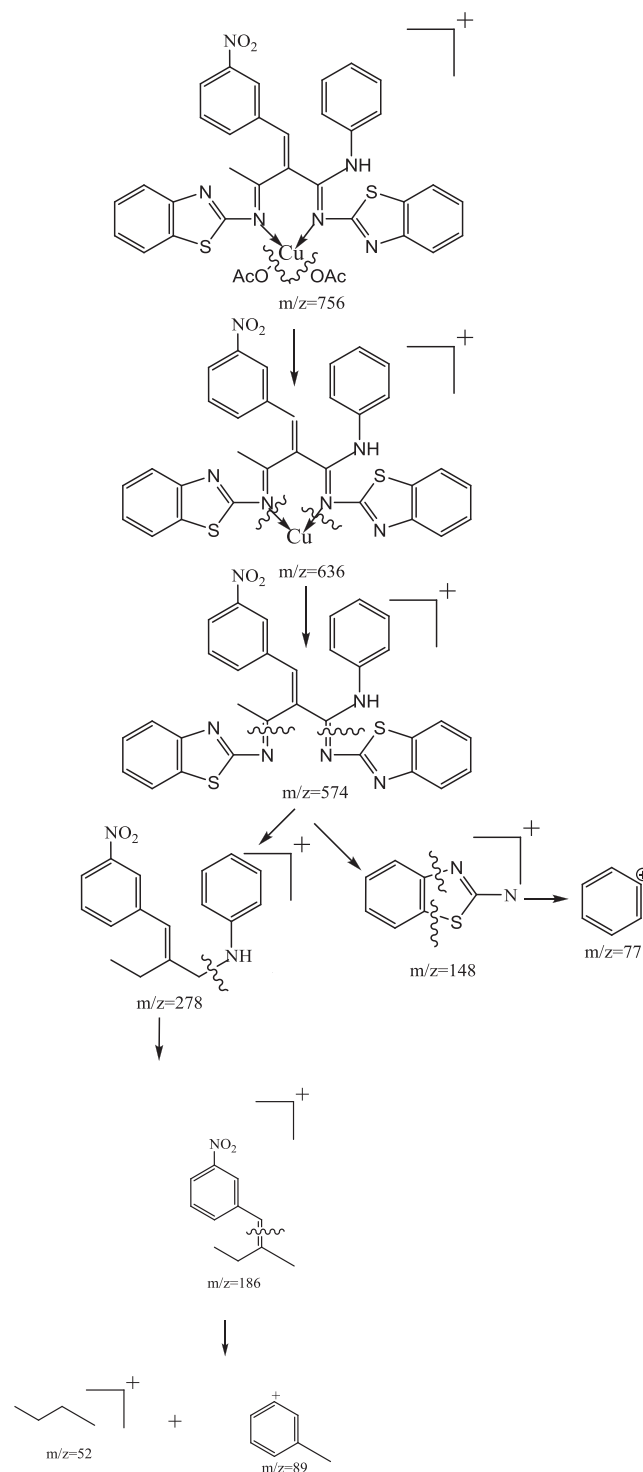
$$\gamma^2 = (g_{\perp} - 2.0027)E / -2\lambda\alpha^2 \quad (4)$$

For the present complex, the observed order  $K_{\parallel}(0.93) > K_{\perp}(0.68)$  implies a greater contribution from out-of plane  $\pi$ -bonding than from in-plane  $\pi$ -bonding in metal–ligand  $\pi$  bonding. The  $A_{\parallel}$  and  $A_{\perp}$  values in the order:  $A_{\parallel}(146) > A_{\perp}(51)$  also indicate that the complex has square planar geometry. The empirical factor  $f = g_{\parallel}/A_{\parallel} \text{ cm}^{-1}$  is an index of tetragonal distortion. Values of this factor may vary from 105 to 135 for small to extreme distortions in square planar complexes and it depends on the nature of the coordinated atoms. The  $f$  values of copper complexes are 153, 151, 146, 148, 144 and 149, indicating significant distortion from planarity.

### 3.5. Mass spectra

The FAB mass spectra of the Schiff bases and their corresponding copper complexes were recorded and compared their stoichiometry compositions (Scheme 2). The  $[\text{CuL}^1(\text{OAc})_2]$  complex shows the molecular ion peak at  $m/z$  757. This molecular ion further by losing two acetate ions gave a fragment ion peak at  $m/z$  638 and these undergo demetallation to form the species  $[\text{L}]^+$  gave fragment ion peak at  $m/z$  575. Cu complexes of  $[\text{CuL}^2(\text{OAc})_2]$ ,  $[\text{CuL}^4(\text{OAc})_2]$ ,  $[\text{CuL}^5(\text{OAc})_2]$  shows molecular ion peak ( $M^+$ ) at  $m/z$  = 745, 745, 745 respectively. Further, the fragmentation of two acetate ions was observed at  $m/z$  = 626, 626, 626. After losing their metal, the corresponding ligands ( $[\text{L}]^+$ ) shows molecular ions peaks at  $m/z$  = 564, 564, 564.

The mass spectrum of Cu(II) complex of  $[\text{CuL}^3(\text{OAc})_2]$  shows a molecular ion peak ( $M^+$ ) at  $m/z$  = 756. The second fragmentation of two acetate ions leads to the formation of ligand moiety of



Scheme 2. Mass fragmentation of copper complex of  $L^3$ .

2-aminobenzothiazole with molecular ion peak at  $m/z$  = 638, resulting from the elimination of metal results ion peak ( $[\text{L}]^+$ ) at  $m/z$  = 574. The mass fragmentation pattern of copper complex of  $L^3$  was shown in Scheme 2.

In case of  $[\text{CuL}^6(\text{OAc})_2]$  complex, the molecular ion peak observed at  $m/z$  = 737. This molecular ion further by losing two acetate atoms gave a fragment ion peak at  $m/z$  = 618 and these demetallation to form the species  $[\text{L}]^+$  gave fragment ion peak at  $m/z$  = 555. Elemental analysis values are in close agreement with the values calculated from molecular formula of these complexes,

which is further supported by the FAB-mass studies of representative complexes.

### 3.6. Thermogravimetric analysis

From thermal analysis, nature of intermediates and final products of the thermal decomposition of coordination compounds can be obtained. From TGA curves, the weight loss was calculated for the different steps and compared with those theoretically calculated for the suggested formulae based on the results of elemental analyses and mass spectra together with the molar conductance measurements. The TGA confirms the formation of CuO as the end products from which the copper content could be calculated and compared with that obtained from the analytical determination.

Thermogravimetric analyses of the copper complexes were recorded. By this Thermogravimetric analysis, we determine the compositional differences as well as to ascertain the nature of associated water molecules. From the thermal investigation (TG/DTG) it is possible to observe that the decomposition occurs for the copper complexes in three ways. All complexes start decomposition at 190–240 °C, suggesting the loss of acetate ions. However, the decomposition at 330–420 °C corresponds to the decomposition of ligands. Above 530–650 °C, copper complexes resulting in CuO as main residue after decomposition steps. The differential thermo-gravimetry (DTG) curve of the representative Cu(II) complex shows three decomposition steps, the first decomposition step in the range 320–410 °C corresponds to loss of acetate molecules, the second decomposition range 580–640 °C range corresponds to loss of 2-aminobenzothiazole moiety, further leaving behind the metal oxide residue above 740–800 °C range.

The results showed that Cu(II) complex of  $L^2$  decompose mainly in three steps. The Cu(II) complex 2 exhibits thermal stability up to 200 °C, which confirms that this complex is free from any types of water molecules. In the first step, two acetate molecules are evolved at 210–230 °C. The complex further decomposes in the second step in the range of 250–410 °C associated with the partial loss of ligand  $L^2$ . In the final decomposition step appeared in the range 460–580 °C corresponding to the complete thermal decomposition of the complexes and the loss of their organic portion results in the formation of CuO as final products. In DTA analysis, An intense exothermic decomposition peaks were observed for  $[CuL^2(OAc)_2]$  at 330 °C, 620 °C, 780 °C shown in Fig. 3. All other copper complexes showed similar thermogram.

The percentage of copper content was calculated from the weight of the ash obtained and compared with those values with the results of atomic absorption spectra (AAS). The copper content in all the complexes was done by elemental analysis agrees well with the thermal studies.

### 3.7. DNA binding experiments

#### 3.7.1. Cyclic voltammetric studies

Cyclic voltammogram of  $[CuL^6(OAc)_2]$  in the absence of DNA showed two segments of cathodic and anodic peaks were shown in Fig. 4. The first segment, cathodic and anodic peaks were observed at  $-0.530$  V and  $-0.390$  V, respectively. This showed reduction from +2 to +1 form sat a cathodic peak potential. Also, the second segments of cathodic peaks and anodic peaks  $E_{pc2}$  and  $E_{pa2}$  at  $-1.522$  V and  $-1.342$  V which corresponds to ligand oxidation and reduction behaviour, respectively.

The cyclic voltammogram of  $[CuL^6(OAc)_2]$  in the presence of different concentration of DNA in the solution of same concentration of the complex causes a considerable decrease in the voltammetric current. In addition, the peak potentials, both  $E_{pa}$  and  $E_{pc}$  as well as  $E_{1/2}$  have a shift to negative potential which is shown in Fig. 5. The decrease extents of the peak currents observed for metal complex

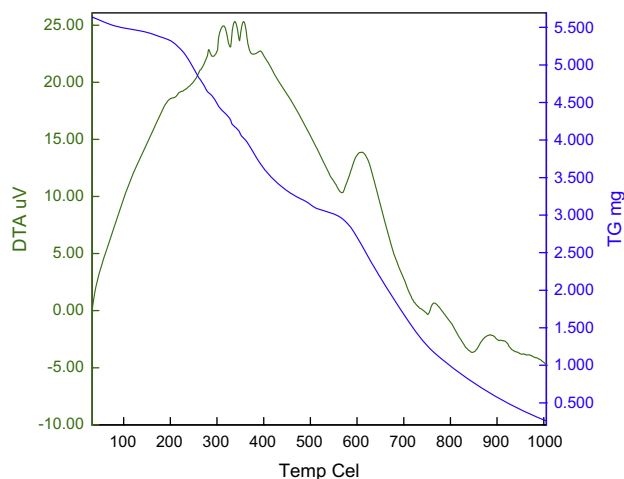


Fig. 3. TGA curve for  $[CuL^2(OAc)_2]$ .

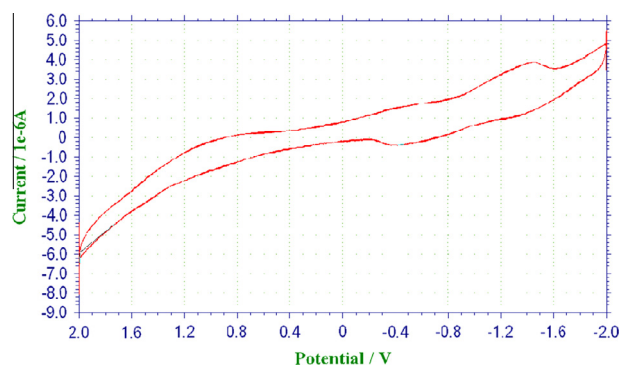


Fig. 4. Cyclic voltammogram of  $[CuL^6(OAc)_2]$  complex.

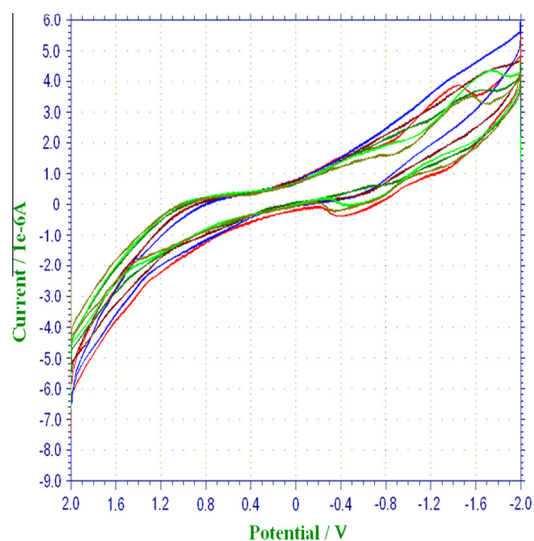


Fig. 5. Cyclic voltammogram of  $[CuL^6(OAc)_2]$  in the presence and absence of different concentrations of DNA.

upon addition of CT-DNA may indicate that the binding affinity of copper complex and thus copper complex interacts with CT-DNA through intercalation binding mode [27]. The electrochemical parameters of the Cu(II) complexes are shown in Table 5. It was concluded that the present ligand systems stabilize the unusual

**Table 5**  
Electrochemical parameters for the interaction of DNA with copper complexes.

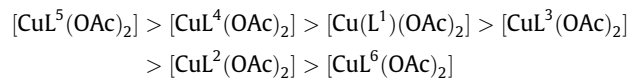
Compound	Redox couple	$E_{1/2}$ (V)		$\Delta E_p$ (V)		$i_{pa}/i_{pc}$
		Free	Bound	Free	Bound	
[CuL <sup>1</sup> (OAc) <sub>2</sub> ]	Cu(II) → Cu(I)	-0.140	-0.517	-0.46	-0.215	1.19
[CuL <sup>2</sup> (OAc) <sub>2</sub> ]	Cu(II) → Cu(I)	-1.432	-1.475	-0.184	-0.250	1.22
[CuL <sup>3</sup> (OAc) <sub>2</sub> ]	Cu(II) → Cu(I)	-0.383	-0.460	-0.144	-0.144	1.15
[CuL <sup>4</sup> (OAc) <sub>2</sub> ]	Cu(II) → Cu(I)	-1.521	-1.615	-0.144	-0.210	1.12
[CuL <sup>5</sup> (OAc) <sub>2</sub> ]	Cu(II) → Cu(I)	-1.405	-1.418	-0.144	-0.180	1.21
[CuL <sup>6</sup> (OAc) <sub>2</sub> ]	Cu(II) → Cu(I)	-0.215	-0.350	-0.144	-0.173	1.25

oxidation states of copper ion during electrolysis. Other copper complexes were also showed similar electrochemical behaviour.

### 3.7.2. Absorption spectral titrations

Electronic absorption spectroscopy is one of the most useful techniques for DNA binding studies of metal complexes. The binding of copper(II) complexes to DNA helix has been characterized through absorption spectral titrations, by following changes in absorbance and shift in wavelength. The experiments were performed by maintaining a constant concentration of the complex while varying the DNA concentration.

In the UV region, the Cu(II) complex of L<sup>1</sup> exhibits a band at ca. 444 nm. With increasing DNA concentration, the absorption bands of the complexes were affected, resulting in a hypochromism tendency and slight shifts to longer wavelengths, which indicates that the Cu(II) complex can interact with DNA (Fig. 6). The observed hypochromism and bathochromism for the Cu(II) complex are large compared to those observed for potential intercalators. The intrinsic binding constant ( $K_b$ ) was obtained by monitoring the change in absorbance with increasing concentrations of DNA for the Cu(II) complexes. The intrinsic binding constant ( $K_b$ ) values of copper complexes of L<sup>1</sup>–L<sup>6</sup> are  $1.6 \times 10^6$ ,  $2.3 \times 10^6$ ,  $1.6 \times 10^6$ ,  $1.9 \times 10^6$ ,  $3.2 \times 10^6$  and  $2.8 \times 10^6$ , respectively and compared with classical intercalator (ethidium bromide-DNA) was found to be  $1.4 \times 10^7 \text{ M}^{-1}$ . The prepared copper complexes are less binding strength than classical intercalator.



These data implies that the compounds interact with CT-DNA by appreciable intercalation binding mode [28]. A similar spectral behaviour was obtained for all other complexes.

### 3.8. Antioxidant assay

Compounds with antioxidant properties could be expected to offer protection in inflammation and lead to potentially effective

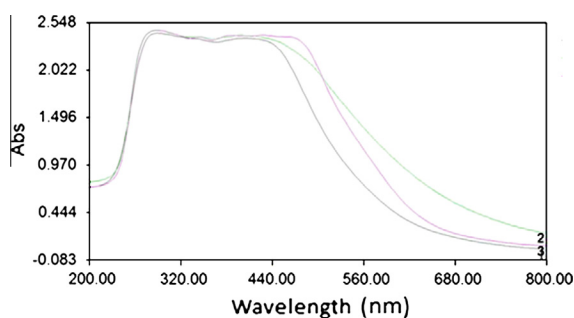


**Fig. 6.** UV Absorption spectrum for [CuL<sup>1</sup>(OAc)<sub>2</sub>] in increasing concentration of CT-DNA.

drugs. Lower IC<sub>50</sub> value, greater the hydrogen donating ability. Copper complex of L<sup>6</sup> showed greater antioxidant activity. Copper complex of L<sup>1</sup> also showed a good antioxidant activity is due to the presence of OH group (efficient hydrogen donors to stabilize the unpaired electrons and there by scavenging free radicals). The introduction of –NO<sub>2</sub> group in the ligand system markedly increases the antioxidant efficiency of the complexes with careful selection of the substituents on the ligands, the antioxidant behaviour of the complexes can be improved.

The synthesized complexes show same antimicrobial and antioxidant activities. The activity was found in the order of [CuL<sup>6</sup>(OAc)<sub>2</sub>] < [CuL<sup>1</sup>(OAc)<sub>2</sub>] < [CuL<sup>3</sup>(OAc)<sub>2</sub>] < [CuL<sup>2</sup>(OAc)<sub>2</sub>] < [CuL<sup>4</sup>(OAc)<sub>2</sub>] < [CuL<sup>5</sup>(OAc)<sub>2</sub>].

### 3.8.1. Superoxide dismutase activity

SODs are metalloenzymes that catalyze the dismutation of the superoxide radical (O<sub>2</sub><sup>-</sup>) into hydrogen peroxide (H<sub>2</sub>O<sub>2</sub>) and molecular oxygen (O<sub>2</sub>), providing an important defense against oxidative damage. SOD catalyzes the dismutation of superoxide through a so called “Ping-Pong mechanism”. First, the metal cation (M<sup>n+</sup>) is reduced to M<sup>(n-1)+</sup> and reoxidized back to M<sup>n+</sup>. Then, superoxide anion converts the tetrazolium salt NBT to NBT-diformazan, a formazan dye. Absorbance is measured at 540 nm using a standard spectrophotometer. Addition of SOD to this reaction reduces superoxide ion levels, thereby lowering the rate of NBT-diformazan formation. SOD activity in the experimental sample is measured as the percent inhibition of the rate of NBT-diformazan formation.

The superoxide dismutase activity (SOD) of the complexes was investigated by the NBT assay method [29]. The chromophore concentration value required to yield 50% inhibition of the reduction of NBT (IC<sub>50</sub>). The IC<sub>50</sub> of present copper complexes was found at the range of 32–45 μmol dm<sup>-3</sup> which are higher than the value exhibited by the native enzyme (IC<sub>50</sub> = 0.04 μmol dm<sup>-3</sup>). All the tested compounds show SOD activity. Similar values obtained for all compounds. The SOD values of Cu(II) complexes were listed in Table 6 and graphically presented in Fig. 7.

In the present study, the higher SOD mimetic activity of copper complexes than that of native enzyme is due to the presence of easily labile acetate ion and also azomethine containing stabilize the Cu(I) complex formed during superoxide dismutation reaction which further reacts with superoxide ion to give hydrogen peroxide. The distorted geometry of these complexes may favour the geometrical change, which is essential for the catalysis as the geometry of copper in the SOD enzyme also changes from distorted square planar geometry. The difference in reactivities of the synthesized complexes may be attributed to the coordination environment and the redox potential of the couple Cu<sup>I</sup>/Cu<sup>II</sup> in copper(II) complexes during the catalytic cycle. The above results also supported from the “f” factor obtained from EPR spectra. The proposed mechanism of SOD activity as follows:



**Table 6**  
Antioxidant activity of Schiff base copper complexes in (μmol dm<sup>-3</sup>).

Compound	IC <sub>50</sub> (μmol dm <sup>-3</sup> )	IC <sub>50</sub> (μmol dm <sup>-3</sup> )
	OH <sup>-</sup>	O <sub>2</sub>
[CuL <sup>1</sup> (OAc) <sub>2</sub> ]	31	33
[CuL <sup>2</sup> (OAc) <sub>2</sub> ]	56	35
[CuL <sup>3</sup> (OAc) <sub>2</sub> ]	33	38
[CuL <sup>4</sup> (OAc) <sub>2</sub> ]	62	32
[CuL <sup>5</sup> (OAc) <sub>2</sub> ]	52	32
[CuL <sup>6</sup> (OAc) <sub>2</sub> ]	25	30
Sodium ascorbate	14.2	14.2
Bovin Erythrocyte	2.1	2.1

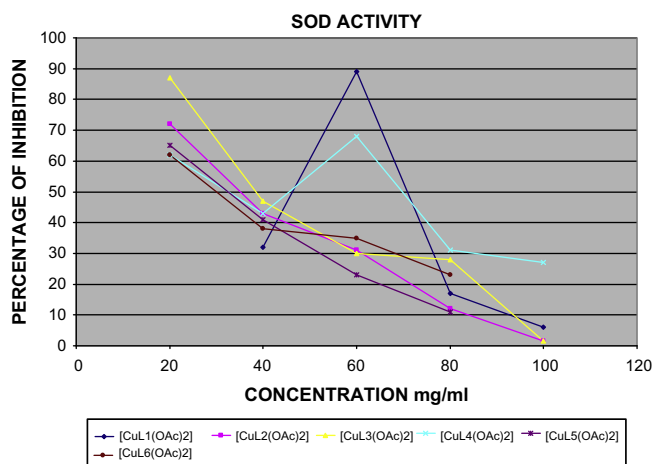


Fig. 7. Superoxide dismutase activity of Cu(II) complexes in ( $\mu\text{mol dm}^{-3}$ ).

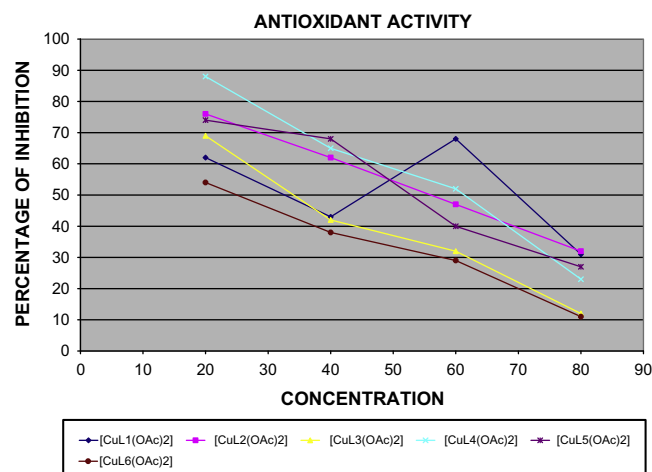


Fig. 8. Anti oxidant activity of Cu(II) complexes in ( $\mu\text{mol dm}^{-3}$ ).

It has been proposed that electron transfer between Cu(II) and superoxide anion radicals occurs through direct binding. As a consequence of this interaction, these ions undergo rapid reduction to Cu(I) with the release of  $\text{O}_2$  molecule. It is assumed that electron transfer between the central metal and  $\text{O}_2^-$  occurs by direct binding [30]. The fast exchange of axial solvent molecules and a limited steric hindrance to the approach of the  $\text{O}_2^-$  in that complexes allow a better SOD mimic.

### 3.8.2. $\text{H}_2\text{O}_2$ scavenging assay

The synthesized compounds scavenged the radical in a concentration dependent manner by causing oxidative damage to biological targets mediated through Fenton type reaction or Haber–Weiss reaction and produce  $\text{OH}^\cdot$  at the site. With increase production of  $\text{OH}^\cdot$ , vigorously damage DNA (with multiple hit effect) and convert them into highly reactive radicals. However it causes damage to the cell even at a very low concentration (20  $\mu\text{l}$ ) because they liberally soluble in aqueous solution and easily penetrate through biological membrane. Results of percentage of free radical scavenging activity are shown in Fig. 8 and the values are tabulated in the Table 6.

### 3.9. Antimicrobial activity

The *in vitro* antimicrobial activities of the investigated compounds were tested against the bacterial species, *Staphylococcus aureus*, *Escherichia coli*, *Klebsiella pneumoniae*, *Proteus vulgaris*, and *Pseudomonas aeruginosa* by disc diffusion method [31,32]. The inhibitions around the antibiotic discs were measured after incubation and Streptomycin was used as standard drug. It was stated that the synthesized copper complexes of 2-aminobenzothiazole derivatives showed more activity than its free ligands.

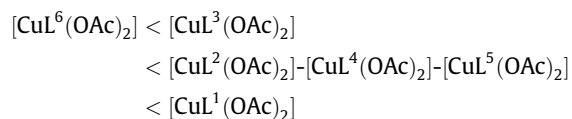
The results with reference to *in vitro* antimicrobial activities of the various copper complexes are listed in Table 7. All the compounds tested revealed moderate to strong antimicrobial activity. Of all the test compounds attempted,  $[\text{CuL}^6(\text{OAc})_2]$  and  $[\text{CuL}^3(\text{OAc})_2]$  showed slightly higher activities against most Gram positive than Gram negative bacteria, but all compounds show strong activity on the yeast cultures when compared with standard drug Streptomycin. The significant activity of the Schiff base ligand may arise from the two imine groups which import in elucidating the mechanism of transformation reaction in biological system. All the metal complexes are found to have higher antibacterial activity against Schiff base ligands. The antibacterial results evidently show that the activity of the Schiff base compounds becomes more pronounced when coordinated to the copper ion. The MIC values

Table 7

MIC values of synthesized compounds and their complexes (in  $\mu\text{g/ml}$ ).

Compound	<i>Staphylococcus aureus</i>	<i>Escherichia coli</i>	<i>Klebsiella pneumoniae</i>	<i>Pseudomonas aeruginosa</i>	<i>Proteus vulgaris</i>
L <sup>1</sup>	16.3	23.8	24.1	23.5	20.2
L <sup>2</sup>	24.6	25.8	28.9	26.5	25.8
L <sup>3</sup>	21.7	17.8	25.9	19.5	22.3
L <sup>4</sup>	24.6	25.8	28.9	26.5	25.8
L <sup>5</sup>	24.6	25.8	28.9	26.5	25.8
L <sup>6</sup>	15.7	17.8	16.9	18.5	17.2
$[\text{CuL}^1(\text{OAc})_2]$	7.3	7.8	7.9	7.4	8.5
$[\text{CuL}^2(\text{OAc})_2]$	8	7.3	8.1	7.6	7.3
$[\text{CuL}^3(\text{OAc})_2]$	7.4	7.3	8	7.5	7.3
$[\text{CuL}^4(\text{OAc})_2]$	8	7.3	8.1	7.6	7.3
$[\text{CuL}^5(\text{OAc})_2]$	8	7.3	8.1	7.6	7.3
$[\text{CuL}^6(\text{OAc})_2]$	6.2	6	6.4	6.7	6
Streptomycin	1.7	1.8	2.3	1.9	1.8

indicate that all the compounds tested exhibit moderate to strong antimicrobial activity on the tested microorganisms. It was observed that increased activity was found in the order of



Copper toxicity has been largely attributed to its redox-properties. It can catalyze the production of highly reactive hydroxyl radicals which can subsequently damage lipids, proteins, DNA and other biomolecules. Therefore, it is possible that copper complexes of highly conjugated curcumin analogs can cause significant disruption in cell membrane (enabling more copper to get through the fungal membrane) leads to extensive damage within the cell.

## 4. Conclusion

Novel Cu(II) complexes with Schiff bases derived from 2-aminobenzothiazole and Knoevenagel condensate of  $\beta$ -ketoanilides have been synthesized and characterized on the basis of elemental analysis, molar conductance, magnetic moment and spectral data. The Schiff bases act as bidentate ligand coordinating through two azomethine nitrogen atoms. Two acetate ions also coordinated to the copper ion. The thermal studies indicate that the metal complexes are thermally more stable compared to the ligand. On the basis of spectral data, copper complexes showed square planar geometry. Antibacterial studies of the ligand and complexes have also been

evaluated which indicate that activity increases on chelation. The complexes show significant SOD activity hence can be considered as good model for SOD activity. DNA binding studies indicated that the Cu(II) complex exhibited stronger binding affinity to DNA through intercalation mode. The higher  $\epsilon$ -values of the d–d band, low  $A_{II}$  values and the reduction potential of these copper complexes suggest that they can serve as synthetic models to mimic natural copper proteins

### Acknowledgement

We express our sincere thanks to the Chancellor, Noorul Islam Centre for Higher Education, Kumaracoil for providing research facilities. This study was funded by CSIR, New Delhi (Grant No. 01(2497)/11/EMR-II).

### Appendix A. Supplementary material

Supplementary data associated with this article can be found, in the online version, at <http://dx.doi.org/10.1016/j.molstruc.2014.01.028>.

### References

- [1] Krishnannair Krishnankutty, Muhammed Basheer, Ummathur, Damodaran Kamalakshy Babu, J. Serb. Chem. Soc. 75 (2010) 639–648.
- [2] C.A. Irena, K. Marijeta, M. Marko, B. Branimir, T. Sanja, P. Gordana, P. Kresimir, K.Z. Grace, J. Med. Chem. 52 (2009) 1744–1756.
- [3] Ruhi Ali, Nadeem Siddiqui, J. Chem. 2013 (2013). Article ID 345198.
- [4] R.M. LoPachin, T. Gavin, B.C. Geohagen, L. Zhang, D. Casper, R. Lekhray, D.S. Barber, J. Neurochem. 116 (2011) 132–143.
- [5] S. Padhye, D. Chavan, S. Pandey, J. Deshpande, K.V. Swamy, F.H. Sarkar, Mini Rev. Med. Chem. 10 (2010) 372–387.
- [6] M. Wang, L.F. Wang, Y.Z. Li, Q.Z. Li, Z.D. Xu, D.M. Qu, Trans. Met. Chem. 26 (2001) 307–310.
- [7] P. Reddy, Y. Lin, H. Chang, Arcivoc. xvi (2007) 113–122.
- [8] Y. Heo, Y. Song, B. Kim, Y.A. Heo, Tetrahedron Lett. 47 (2006) 3091–3094.
- [9] F. Piscitelli, C. Ballatore, A. Smith, Bioorg. Med. Chem. Lett. 20 (2010) 644–648.
- [10] Safaa Eldin H. Etaiwa, Dina M. Abd El-Aziza, Eman H. Abd El-Zaherb, Elham A. Ali, Spectrochim. Acta Part A Mol. Biomol. Spectrosc. 79 (2011) 1331–1337.
- [11] D.P. Fairlie, M.W. Whitehouse, Drug Des. Discov. 8 (1991) 83–102.
- [12] D.E. Metzler, M. Ikwa, E.E. Snell, J. Am. Chem. Soc. 76 (1954) 648–652.
- [13] I. Sakyar, E. Logoglu, S. Arslan, N. Sari, N.S. Akiyan, BioMetals 17 (2004) 115.
- [14] Guan-Yeow Yeap, Boon-Teck Heng, Nur Faradiana, Raihana Zulkifly, Masato M. Ito, Makoto Tanabe, Daisuke Takeuchi, J. Mol. Struct. 1012 (2012) 1–11.
- [15] Ahmed A. El-Sherif, J. Solution Chem. 41 (2012) 1522–1554.
- [16] F. Gonzalez-Vilchez, R. Vilaplana,  $^{29}\text{Cu}$  chemotherapeutic copper compounds, in: M. Gielen, E.R.T. Tiekink (Eds.), Metallotherapeutic Drugs and Metal-Based Diagnostic Agents, John Wiley & Sons, New York, NY, USA, 2005, pp. 219–236 (Chapter 12).
- [17] F. Tisato, C. Marzano, M. Porchia, M. Pellei, C. Santini, Med. Res. Rev. 30 (2010) 708–749.
- [18] Y. Wang, X. Zhang, Q. Zhang, Z. Yang, Biometals 23 (2010) 265–273.
- [19] M. Robert Silverstein, X. Francis Webster, Spectroscopic Identification of Organic Compounds, sixth ed., Wiley, India, 2009.
- [20] M.A. Neelakantan, M. Esakkiammal, S.S. Marriappan, J. Dharmaraja, T. Jeyakumar, Indian J. Pharm. Sci. 72 (2010) 216–222.
- [21] N. Raman, J. Joseph, Russ. J. Inorg. Chem. 55 (2010) 1064–1074.
- [22] N. Raman, S. Sobha, M. Selvaganapathy, R. Mahalakshmi, Spectrochim. Acta Part A Mol. Biomol. Spectrosc. 96 (2012) 698–708.
- [23] P.K. Ray, B. Kauffman, Inorg. Chim. Acta 173 (1990) 207–223.
- [24] A. Vijayaraja, R. Prabua, R. Suresh, C. Sivaraj, N. Raman, V. Narayanan, J. Coord. Chem. 64 (2011) 637–650.
- [25] M. Mariappan, B.G. Maiya, Eur. J. Inorg. Chem. 2005 (2005) 2164–2173.
- [26] Jorge Manzur, Hector Mora, Andres Vega, Evgenia Spodine, Diego Venegas-Yazigi, Maria Teresa Garland, M. Salah El Fallah, Albert Escuer, Inorg. Chem. 46 (2007) 6924–6932.
- [27] T. Sathiya Kamatchi, N. Chitrapriya, H. Lee, C.F. Fronczek, F.R. Fronczek, K. Natarajan, Dalton Trans. 41 (2012) 2066–2077.
- [28] X.L. Zhao, M.J. Hana, A.G. Zhanga, K.Z. Wang, J. Inorg. Biochem. 107 (2012) 104–110.
- [29] L.M. Gaetke, C.K. Chow, Toxicology 189 (2003) 147–163.
- [30] C.W. Yaw, W.T. Tan, W.S. Tan, C.H. Ng, W.B. Yap, N.H. Rahman, Mohamed Zidan, Int. J. Electrochem. Sci. 7 (2012) 4692–4701.
- [31] N. Chitrapriya, Y.J. Jang, S.K. Kim, H. Lee, J. Inorg. Biochem. 105 (2011) 1569–1575.
- [32] C.H. Collins, P.M. Lyre, J.M. Grange, Microbiological Methods, sixth ed., Butterworth Co. Ltd., London, 1989.